

# Coulomb Blockade and Hopping Conduction in Graphene Quantum Dots Array

Daeha Joung<sup>1,2</sup>, Lei Zhai<sup>1,3</sup>, and Saiful I. Khondaker<sup>1,2\*</sup>

<sup>1</sup> Nanoscience Technology Center, <sup>2</sup> Department of Physics, <sup>3</sup> Department of Chemistry,  
University of Central Florida, Orlando, Florida 32826, USA.

\* To whom correspondence should be addressed. E-mail: saiful@mail.ucf.edu

We show that the low temperature electron transport properties of chemically functionalized graphene can be explained as sequential tunneling of charges through a two dimensional polydispersed array of graphene quantum dots (GQD). Below 15 K, a total suppression of current due to Coulomb blockade (CB) through GQD array was observed. Temperature dependent current-gate voltage characteristics show Coulomb oscillations with energy scales of 6.2-10 meV, while resistance data exhibit an Efros-Shklovskii variable range hopping arising from CB and structural and size induced disorder.

Graphene has ignited intense research interest for their potential applications in nanoelectronics as well as model systems to investigate novel quantum transport phenomenon in confined geometries [1-4]. Recently, much attention has been focused on creating an energy band gap for conventional semiconductor device applications. This energy band gap can be achieved through quantum confinement by patterning graphene into nano-ribbon [5] as well as via chemical functionalization by means of oxidation and reduction of graphene sheets [6-7] which creates nanoscale domains. The transport studies of the former have been explained using Anderson localization [8] or Coulomb blockade effects [9-10]. The transport properties of the latter, reduced graphene oxide (RGO) sheets, has not been well understood due to the complexity of both structural, edge and size disorders [11-12] although it offers a convenient route for the high throughput fabrication of graphene sheets via solution processing for device applications [6]. Theoretical and experimental investigations of RGO have provided evidence of tunable band gap by varying the reduction process [7, 12].

Although RGO shows the potential to tune the band gap in graphene, it is still not easily predictable from either theoretical or experimental standpoint how the disorders affect the electronic transport properties. The structural characterizations of RGO show that it consists of ordered nanocrystal graphitic regions surrounded by areas of oxidized carbon atoms, point defects, and topological defects [11-14]. Previous electrical transport studies of RGO in limited temperature range show 2D Mott variable range hopping [11, 15]. This model neglects the Coulomb interaction between localized graphitic domains. However, recent study of individual 10 nm sized graphene quantum dots which show room temperature Coulomb blockade (CB) [2], suggests that CB and Coulomb interaction should be dominant in low temperature transport studies of RGO as it consists of many nanoscale graphene domains.

In this letter, we show clear evidence that the low temperature electron transport properties of RGO sheet is indeed dominated by Coulomb blockade and interaction effect, and can be modeled as a transport through an array of polydispersed graphene quantum dots (GQD) where graphitic domains acts like QDs while oxidized domain behave like tunnel barriers between QDs. From the temperature dependent transport data, we obtain GQD sizes to vary from 5-8 nm and demonstrate that the wave function is localized within each GQD.

RGO sheets were synthesized through a reduction of GO prepared by modified Hummers method. The devices were fabricated via dielectrophoretic assembly of RGO sheets between the prefabricated gold source and drain electrodes. Details of the synthesis and device assembly were presented in our previous publication [16]. In brief, oxidized graphite in water was ultrasonicated to achieve GO sheets followed by centrifugation for 30 minutes at 3000 rpm to remove any unexfoliated oxidized graphite. The pH of GO dispersion in water (0.1 mg/ml) was adjusted to 11 using a 5 % ammonia aqueous solution. Hydrazine hydrate was added and the solution was heated for 1 hour at 90 °C. Devices were fabricated on heavily doped silicon (Si) substrates capped with a thermally grown 250 nm thick SiO<sub>2</sub> layer. Source and drain electrode patterns of 500 nm x 500 nm (channel length x width) were defined by electron beam lithography (EBL) followed by thermal deposition of 5 nm thick Cr and 20 nm thick Au and standard lift-off. A small drop of RGO solution was placed onto the electrodes pattern. An AC voltage of approximately 3  $V_{p-p}$  at 1 MHz was applied for 20-30 seconds after which the solution droplet was blown off by nitrogen gas. Figure 1(a) inset shows a tapping-mode AFM image of a representative device. From the thickness measurement, we estimate that 2 to 10 layers of RGO sheets have been assembled in the channel. The devices were then bonded and loaded into a variable temperature cryostat for temperature dependent electronic transport measurements. A total of 8 samples were investigated.

Figure 1 (a) shows current-voltage ( $I$ - $V$ ) characteristics of a representative device at 30, 25, 20, 15, 10 and 4.2 K. The backgate voltage  $V_g$  was kept fixed at 0 V. With decreasing temperatures, the  $I$ - $V$  curves become increasingly nonlinear. However, all the curves are highly symmetric. As the temperature is lowered to less than 15 K, a complete suppression of current below a threshold voltage ( $V_t$ ) was observed. Similar current suppression was observed in a previous study of individual GO devices with highly-asymmetric  $I$ - $V$  curve and was explained by a Schottky barrier (SB) between metallic contact and GO [17]. However, our  $I$ - $V$  curves are highly symmetric giving evidence that the current suppression and symmetric nonlinear behavior is not due to SB. Rather, such current suppression is due to CB of charges, as at low temperatures there is not enough energy for the charges to overcome Coulomb charging energies of the QD array formed by graphitic domains. In this scenario, the RGO sheet behaves as a GQD array where graphitic domains are quantum dots, and oxidized domains are tunnel barriers.

Theoretical studies of QD arrays by Middleton and Wingreen (MW) predicts that

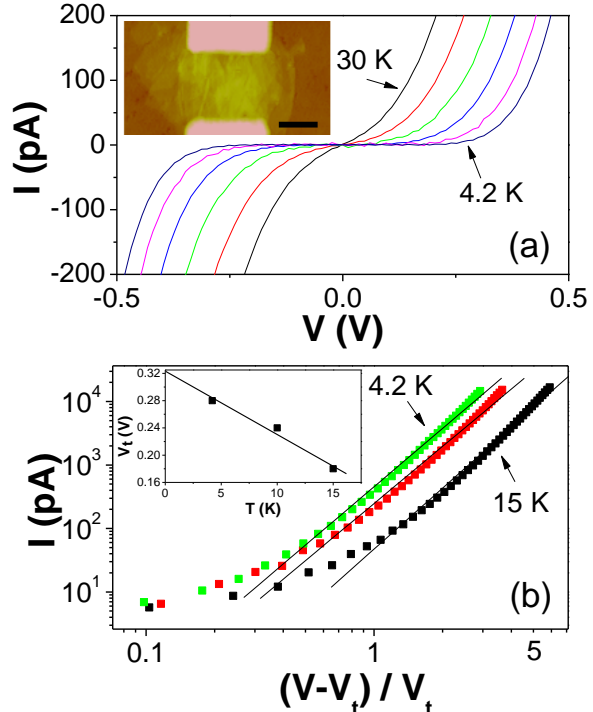


FIG. 1. (Color online) (a)  $I$ - $V$  characteristics of a representative RGO device at temperatures 30, 25, 20, 15, 10 and 4.2 K. Below 15 K, the current is zero for  $V < V_t$  due to coulomb blockade of charges. Inset: AFM image of the device. Scale bar = 500 nm. (b)  $I$  vs.  $(V-V_t)/V_t$  curves plotted in a log-log scale. Slope of the curves gives the value of exponent  $\alpha = 2.8$ . Inset shows the dependence of  $V_t$  on  $T$ . From the plot,  $V_t(0)$  was estimated as 0.32 V.

the  $I$ - $V$  curves should follow the relation  $I \propto [(V - V_t)/V_t]^\alpha$  for  $V > V_t$ , where  $\alpha$  is the scaling exponent that depends on the dimensionality of the arrays [18]. Figure 1(b) shows  $I$  plotted versus  $(V - V_t)/V_t$  in a log-log scale using  $V_t = 0.18, 0.24, 0.28$  V at  $T = 15, 10,$  and  $4.2$  K respectively. The symbols are the experimental data points while the solid lines are fits to the above equation. From the fits, we obtain  $\alpha = 2.8 \pm 0.1$ . For a two-dimensional array of nanoparticles, the theoretical value of  $\alpha$  was predicted as 1.6 while numerical simulations yielded as 2.0 [18]. However, in previous experimental studies of two dimensional metal nanocrystal arrays, the exponent  $\alpha$  was reported to vary from 2 to 2.5, while for quasi 2D system with multilayered nanoparticles the value was 2.6 to 3.0 [19, 20]. Our value of  $\alpha$  is in agreement with charge transport in a quasi 2D QD array and is expected since we have up to 10 layers of RGO sheets. Figure 1(b) inset shows  $V_t$  plotted versus  $T$  from which we see that  $V_t$  increases linearly with decreasing  $T$ . Extrapolation of the  $V_t$  plot to 0 K provides the global threshold voltage  $V_t(0) = 0.32$  V. Similar  $I$ - $V$  curves were observed for all 8 samples with  $\alpha$  varying from 2.52 to 2.80 and  $V_t(0)$  varying from 0.32 to 0.42. For an array of nanoparticles of uniform size,  $V_t(0)$  can be expressed as  $V_t(0) \approx E_c(\beta N)$  where  $E_c$  is charging energy of a QD,  $\beta$  is a prefactor whose value depends on the dimensionality and arrays geometry (for a 2D array  $\beta = 0.3$ ), and  $N$  is the number of QDs in the conduction path [18, 21]. From here, we can estimate the number of GQDs in our array contributing in the charge transport, however, we need to estimate  $E_c$  first.

In order to calculate the  $E_c$  of the GQDs, we measured  $I$  as a function of gate voltage ( $V_g$ ) at temperatures  $T = 4.2$  to 120 K. This is shown in Fig. 2. The reproducible peaks in  $V_g$  correspond to single electron tunneling (Coulomb oscillations) through graphene QD arrays. The bias voltage was kept fixed at  $V = 0.3$  V.

The peaks in  $V_g$  are not periodic, in agreement with the sequential tunneling of charges through multiple QDs. Such Coulomb oscillations have never been observed in previous studies of 2D metallic or magnetic QD array systems. This may be due to the fact that, the density of states (DOS) in those systems is higher and gate voltage has negligible effect in DOS. While in RGO, the DOS is low allowing the gate to tune the DOS giving rise to Coulomb oscillations. As the temperature is increased from 4.2 K to 120 K, two important features can be noticed. The peaks around  $V_g = 0$ , washes out around 70 K corresponding to a thermal energy of 6.2 meV. This is more clearly shown in Fig. 2 (b), where we plot  $-10 < V_g < 10$  V regime up to  $T = 70$  K of Fig. 2 (a). The other peaks survive up to 120 K (Fig. 2 (c)) which corresponds to a thermal energy of 10 meV.

From the semi classical orthodox theory of CB, the charging energy  $E_c$  required to add an electron to a QD is given

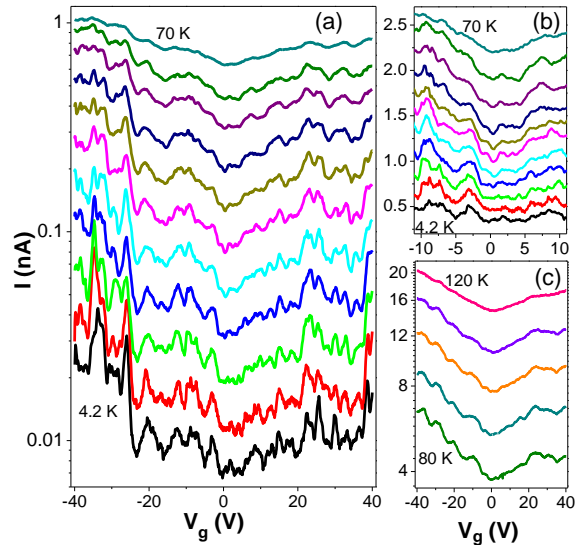


FIG. 2. (Color online) (a) Current ( $I$ ) as a function of gate voltage ( $V_g$ ) for  $T = 4.2, 10, 15, 20, 25, 30, 35, 40, 50, 60$  and  $70$  K. The reproducible peaks correspond to Coulomb oscillations. For the unified view,  $I$  at 50, 60 and 70 K were divided by 1.5, 2, and 3.5. At 70 K, peaks around  $V_g = 0$  were washed out. This is more clearly shown in (b). For clarity, curves from bottom to top in (b) were multiplied by a factor of 49, 41, 31, 23, 17, 12.5, 9, 6.7, 3.5, and 2.2 respectively. (c)  $I$ - $V_g$  curves for  $T = 80$ -120 K with a step of 10 K. At 120 K, all the oscillations were washed out. Bias voltage was 0.3 V.

by,  $E_c = e^2/2C_\Sigma$ , where  $C_\Sigma$  is the total capacitance which depends on the size of each QD and their inter-dot separation. In order to observe the coulomb oscillations,  $E_c$  should be larger than thermal energy  $k_B T$ . Therefore our temperature dependent data gives an estimate of  $E_c$  to vary from 6.2 – 10 meV. We suggest that this variation in charging energy is indicative of a large size distribution of GQDs in the transport pathway (polydispersed GQD array).

Using the  $E_c$  values, the total capacitance is estimated to vary from  $C_\Sigma = 8\text{-}13$  aF. Neglecting the size variation for the time being,  $C_\Sigma$  can also be estimated from the geometrical consideration and can be written as  $C_\Sigma = C_g + 9C$ , where  $C_g \approx 4\pi\epsilon\epsilon_0 r$  and  $C \approx 2\pi\epsilon\epsilon_0 \ln[(r+d)/d]$  are self-capacitance and mutual capacitance of QDs respectively [19]. Here,  $r$  is the radius of GQD,  $2d$  is spacing between QDs,  $\epsilon$  is the dielectric constant of RGO,  $\epsilon_0$  is value for permittivity of vacuum, and the factor 9 is the average number of nearest neighbors of each QD in a quasi 2D system [22]. The value of  $\epsilon_r$  can be calculated by using  $\epsilon_r = n^2 - k^2$ , where  $n$  and  $k$  are refractive index and extinction coefficient of RGO film respectively. Using the values of  $n$  and  $k$  in the thermally reduced GO, the calculated value of dielectric constant  $\epsilon_r$  estimated to be around 3.5 [23]. By comparing experimental value and theoretical equation of  $C_\Sigma$ , we can calculate the value of  $r = 2.5$  to 4 nm (domain size 5 – 8 nm) using  $d = 0.75$  nm. These values obtained from electron transport spectroscopy is in excellent agreement with microscopic studies using transmission electron microscopy (TEM) which highlighted that the size of graphitic regime varies from 3 to 10 nm [13, 14]. We used  $d = 0.75$  nm as the recent TEM study show that the typical size of oxidized or defective region varies from 1-2 nm [14] giving an average value for  $2d = 1.5$  nm. The calculated domain size of GQD is also in good agreement with the domain size obtained from our Raman study [24].

We can now estimate the number of GQDs in the conduction pathway ( $N$ ) of the array using the global threshold voltage formula  $V_t(0) \approx E_c(\beta N)$ . Using an average value of  $E_c$  to be 8.1 meV, we estimate  $N = 131$ . This is a slight over estimation considering the average size of each dot as 6.5 nm and average inter-dot separation of 1.5 nm, we would expect about 65 QD in 500 nm channel. The discrepancies may be due to the fact that we are using MW formula which neglects size disorder which can have a great influence in  $V_t$ . For example, if we consider that the smallest dot size has the most influence in the determination of  $V_t$  as pointed out by Muller et al [25], then we obtain a more reasonable value of  $N \sim 90$ .

In order to further understand the electronic transport mechanism of the GQD array, we study the temperature dependence of the resistance of our devices. Temperature-dependence of resistance can provide evidence about size distribution and the degree of disorder of the GQD array. Figure 3 (a) shows the resistance ( $R$ ) vs. temperature ( $T$ ) plot in the temperature range of 250-30 K for one of the devices. It can be seen that  $R$  changes by over three orders of magnitude over this temperature range.  $R$  was calculated by measuring the current at a constant  $V = 100$  mV as the temperature was lowered (see solid line in Fig 3 (a)). We have also measured  $I$ - $V$  curves at a few selected temperatures and obtained the  $R$  values from the Ohmic part of the  $I$ - $V$  curves (open circle in Fig. 3(a)). The  $R$  values of the two measurements were in agreement. Below 30 K, the  $I$ - $V$  curves were non-Ohmic under 100 mV and those data were discarded from this plot.

According to the QD array model, if QDs are monodispersed, the temperature dependence of resistance should follow thermally activated behavior  $R \sim R_0 \exp(E_0/k_B T)$  [19], while if the nanocrystals have significant size variation (polydispersed) it should follow Efros-Shklovskii variable range hopping (ES-VRH),  $R \sim R_0 \exp(T_0/T)^{1/2}$  [19,26], where  $T_0$  is a constant related to the disorderness of the material. Fitting resistance data with different behavior can be tricky and the same data can often fit with several behaviors (such as  $T^{-1}$ ,  $T^{-1/2}$ ,  $T^{-1/3}$ ). A better

way of determining the exponent value is to consider a generalized formula  $R(T)=R_0 \exp(T_0/T)^p$  and then calculate the value of  $p$  from  $\ln W = A - p \ln T$ , where  $W = -\partial \ln R(T)/\partial \ln T = p(T_0/T)^p$  is the reduced activation energy and  $A$  is a constant [27].

Figure 3 (b) shows  $\ln W$  plotted versus  $\ln T$ . From the slope (indicated by red line) of this curve, we obtain  $p = 0.48 \pm 0.05$ , which is consistent with ES VRH over the whole temperature range. For comparison, we have also plotted two lines for  $p = 1/3$  and  $p = 1$  which unequivocally show that the transport is only described by  $p = 1/2$  model. In previously reported data on single layer RGO devices, 2D Mott VRH ( $p = 1/3$ ) was reported [11, 15]. This may be due to limited temperature range of the data where it might be possible to fit the same data with both  $T^{-1/2}$  and  $T^{-1/3}$  law. Our self consistence analysis of the resistance data that span over three orders of magnitude clearly indicates that there is no conduction mechanism other than the ES VRH for the whole temperature ranges. The characteristics of ES VRH model is in strong agreement with what is expected for a polydispersed GQD array.

The ES VRH indicates strong localization of wave functions in GQDs. Further analysis of ES VRH data allows us to calculate the localization length  $\xi$  by plotting  $R$  against  $T^{-1/2}$  in a semi-log scale. This is shown in Fig. 3 (c) which shows a straight line as expected. From the slope of this curve, we obtain  $T_0 = 4200$  K.  $T_0$  is related to  $\xi$  through  $T_0 = [(2.8e^2 / 4\pi\epsilon\epsilon_0 k_B \xi)]$  [26]. The calculated value of  $\xi$  is about 3.5 nm which is comparable to the calculated GQD sizes, indicating strong localization of the wave function inside each graphitic domain. Similar ES-VRH was observed for all the 8 samples with  $\xi$  varying from 2.3-3.8 nm.

All the measurements and analysis presented here clearly demonstrate that the low temperature charge transport properties of RGO can be modeled as due to a CB and hopping conduction through a polydispersed GQD arrays. From our temperature dependence data, we obtain the GQD sizes to vary from 5 to 8 nm, in excellent agreement with previous TEM study. Observation of ES VRH with a localization length is comparable to the size of each GQD show that Coulomb interaction and size disorder play an important role.

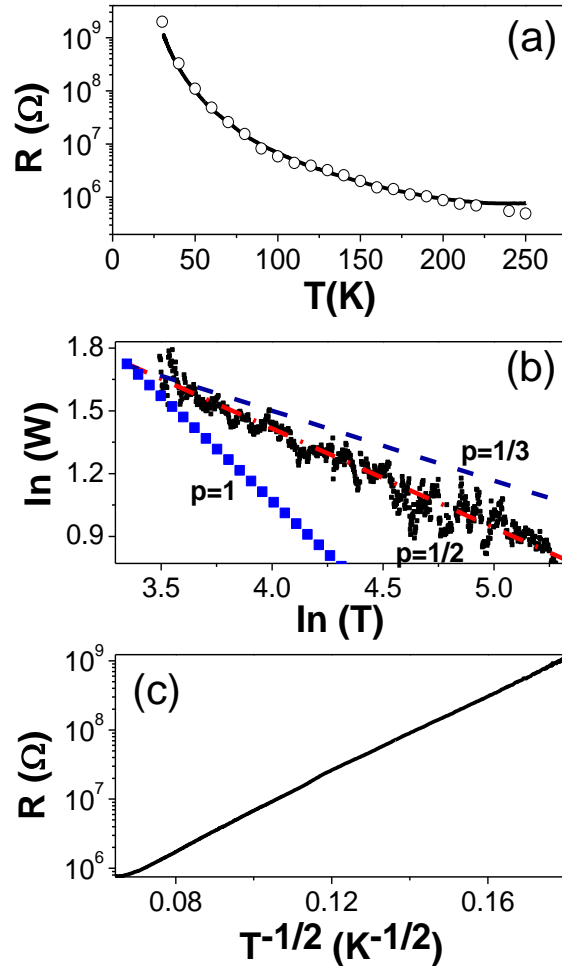


FIG. 3. (Color online) (a) Resistance ( $R$ ) versus temperature ( $T$ ) in a semi-log scale showing four orders of change in  $R$  for  $T = 30$ -250 K. The solid line represents  $R$  measured at a fixed  $V=100$  mV as  $T$  was decreased. The open symbols show  $R$  measured from the Ohmic part of the  $I$ - $V$  curves measured at a few selected  $T$ . (b) Reduced activation energy  $W = -\partial \ln R(T)/\partial \ln T = p(T_0/T)^p$  plotted vs  $T$  on a log-log scale. From the slope of this plot we obtain  $p=0.48 \pm 0.05$  corresponding to the ES-VRH. For a comparison we also show lines with  $p = 1$  (activated hopping) and  $p = 1/3$  (Mott VRH). Our data does not fit with those model. (c)  $R$  in log scale as a function of  $T^{-1/2}$ . From the slope we obtain  $T_0 = 4200$  K.

We thank Eduardo Mucciolo for useful discussions. This work has been partially supported by U.S. NSF under Grant No. ECCS 0748091 to S.I.K. and under Grant No. DMR 0746499 to L.Z.

## References

1. K.S. Novoselov *et al.*, Science **306**, 666 (2004).
2. A. K. Geim and K. S. Novoselov, Nature Mater. **6**, 183 (2007).
3. Y. Zhang *et al.*, Nature **438**, 201 (2005).
4. C. Berger *et al.*, J. Phys. Chem. B **108**, 19912 (2004)
5. M.Y. Han *et al.*, Phys. Rev. Lett. **98**, 206805 (2007); M. Y. Han, J. C. Brant, and P. Kim Phys. Rev. Lett. **104**, 056801 (2010).
6. S. Stankovich *et al.*, Nature **442**, 282 (2006); H.C. Schniepp *et al.*, J. Phys. Chem. B **110**, 8535 (2006).
7. J. Yan *et al.*, Phys. Rev. Lett **103**, 086802 (2009).
8. E. R. Mucciolo, A. H. Castro Neto, and C. H. Lewenkopf, Phys. Rev. B **79**, 075407 (2009); I. Martin and Y. M. Blanter, Phys. Rev. B **79**, 235132 (2009).
9. F. Sols, F. Guinea, and A. H. CastroNeto, Phys. Rev. Lett. **99**, 166803 (2007).
10. C. Stampfer *et al.*, Phys. Rev. Lett. **102**, 056403 (2009).
11. C. Go ´mez-Navarro *et al.*, Nano Lett. **7**, 3499 (2007).
12. K. A. Mkhoyan *et al.*, Nano Lett. **9**, 1058 (2009); C. Mattevi *et al.*, Adv. Funct. Mater. **19**, 2577 (2009).
13. K. Erickson *et al.*, Adv. Funct. Mater. In press DOI: 10.1002/adma.201000732
14. C. Go ´mez-Navarro *et al.*, Nano Lett. **10**, 1144 (2010).
15. A. B. Kaiser *et al.*, Nano Lett. **9**, 1787 (2009). G. Eda *et al.*, J. Phys. Chem. C **113**, 15768 (2009).
16. D. Joung *et al.*, Nanotechnology **21**,165202 (2010).
17. X. Wu *et al.*, Phys. Rev. Lett. **101**, 026801 (2008).
18. A. A. Middleton and N. S. Wingreen, Phys. Rev. Lett. **71**, 3198 (1993).
19. C. T. Black *et al.*, Science **290**, 1131 (2000).
20. M. G. Ancona *et al.*, Phys. Rev. B **64**, 033408 (2001); P. Beecher *et al.*, Adv. Mater. **17**, 1080 (2005); R. P. Tan *et al.*, Phys. Rev. B **79**, 174428 (2009),
21. R. Parthasarathy, X. M. Lin, and H. M. Jaeger, Phys. Rev. Lett. **87**, 186807 (2001).
22. For 2 D and 3 D hexagonal arrays, each nanocrystal has between 6 and 12 nearest neighbors. MW model showed that our device is quasi 2 D GQD layers; so on average of each GQD has ~ 9 nearest neighbors.
23. I. Jung *et al.*, J. Phys. Chem. C **112**, 8499 (2008).
24. D. Joung *et al.*, App. Phys. Lett. **97**, 093105 (2010). An estimate of graphene domain size can also be obtained by comparing the intensity of D and G peaks of the Raman spectrum of the RGO sheets using empirical Tuinstra-Koenig relation [F. Tuinstra, and J. L. Koenig, J. Chem. Phys. **53**, 1126 (1970)]. We obtained a mean domain size of ~ 4 nm from our Raman data.
25. Muller, K. Katayama, and H. Mizuta, J. Appl. Phys. **15**, 5603 (1998).
26. A. L. Efros and B. I. Shklovskii, in Electron-Electron Interactions in Disordered Systems, edited by A. L. Efros and M. Pollak (North-Holland, Amsterdam, 1985), p. 409.
27. A. G. Zabrodskii, and K. N. Zeninova, Sov. Phys. JETP **59**, 425 (1984); S. I. Khondaker *et al.*, Phys. Rev. B **59**, 4580 (1999).